nature neuroscience

Dynamics of excitation and inhibition underlying stimulus selectivity in rat somatosensory cortex

W Bryan Wilent & Diego Contreras

Neurons in sensory systems respond to stimuli within their receptive fields, but the magnitude of the response depends on specific stimulus features. In the rodent whisker system, the response magnitude to the deflection of a particular whisker is, in most cells, dependent on the direction of deflection. Here we use *in vivo* intracellular recordings from thalamorecipient neurons in layers 3 and 4 of the rat barrel cortex to elucidate the dynamics of the synaptic inputs underlying direction selectivity. We show that cells are direction selective despite a broadly tuned excitatory and inhibitory synaptic input. Selectivity emerges from a direction-dependent temporal shift of excitation relative to inhibition. For preferred direction deflections, excitation precedes inhibition, but as the direction diverges from the preferred, this separation decreases. Our results illustrate a mechanism by which the timing of the synaptic inputs, and not their relative peak amplitudes, primarily determine feature selectivity.

Selectivity for stimulus properties is a defining characteristic of single neurons at all levels of sensory systems. In primary sensory cortices, especially in thalamic input layers, selectivity probably originates from the anatomically precise convergence of thalamic inputs. However, the dynamics of sensory-triggered synaptic inputs may vary between, or even within, primary sensory cortices. In primary visual cortex, it has been shown that a diversity of input organization strategies may underlie selectivity[1], and different strategies may be localized to subregions of cortex[2]. In primary auditory cortex, excitation and inhibition are seemingly balanced, and tuning is largely a product of the tuning of the total synaptic input[3]. Selectivity may be sharpened by coactivated feed-forward inhibition, which ultimately dominates the membrane potential (V_m)[4,5]. It has been hypothesized that inhibition sharpens selectivity by limiting the ability of nonoptimal or weaker inputs to evoke an action potential[1,6,7], and this mechanism may be used in all sensory cortices[2,6].

Neurons in the trigeminal nucleus, thalamus and cortex of the rodent whisker system are sensitive to the angular direction of whisker deflection[8,9]. In layer 4 of barrel cortex, it has recently been shown that minicolumns[10] exist, spanning 75–100 μm in the horizontal dimension, in which convergent thalamic inputs share a similar direction preference[11]. However, given the degree of dendritic arborization of barrel neurons (>200 μm)[12,13], the horizontal spread of thalamocortical axonal collaterals (>200 μm)[14] and the recurrent corticocortical connectivity[13,15], it is surprising that direction selectivity is preserved, or even slightly enhanced, in single cells within the barrel. Here, for layer 4 barrel cortex neurons, we estimated the excitatory and inhibitory components of the synaptic response to whisker deflection in different directions. We found that the amplitudes of both synaptic conductances were only weakly selective for direction and that both were largest for the preferred direction. In contrast, their relative timing was clearly direction dependent. Early in the response, the balance of the excitatory and inhibitory inputs was clearly direction dependent, but by 7–10 ms, when the total synaptic input was largest, the balance of the inputs was direction independent. Thus, our results indicate that the temporal dynamics of the synaptic inputs is the critical mechanism determining direction selectivity.

RESULTS

Quantification of direction selectivity *in vivo*

We recorded intracellularly ($n = 37$) from neurons in the main thalamorecipient layers (deep layer 3 and layer 4; depth of 450–850 μm) of the posteromedial barrel subfield of primary somatosensory cortex, the cortical region associated with the whiskers on the face. All cells included in the database presumably received monosynaptic thalamic inputs as judged by the latency to onset of their synaptic response (<7 ms) to a whisker deflection. For each cell, the principal whisker was determined and repeatedly deflected in eight randomly interleaved directions separated by 45° (**Fig. 1a**). Single-trial responses to whisker deflection consisted of a robust synaptic response occasionally leading to one or two spikes (**Fig. 1a**). The spike output was quantified by generating peristimulus spike histograms (PSTH; **Fig. 1a**). Barrel cortex neurons recorded intracellularly at the resting membrane potential (V_m) *in vivo* under anesthesia characteristically respond with very few spikes per stimulus[5,16]; therefore, spike output was increased with slight DC depolarization (range = 0.1 to 0.4 nA) to a discharge level more comparable with the awake-behaving state[17]. In the example cell in **Figure 1**, the rostral direction (180°) was deemed the preferred direction, as it evoked the most spikes per stimulus (0.88 spikes per stimulus at −65 mV and +0.2 nA) and the largest synaptic

Department of Neuroscience, University of Pennsylvania School of Medicine, 215 Stemmler Hall, Philadelphia, Pennsylvania 19106, USA. Correspondence should be addressed to D.C. (diegoc@mail.med.upenn.edu).

Received 22 April; accepted 19 August; published online 11 September 2005; doi:10.1038/nn1545

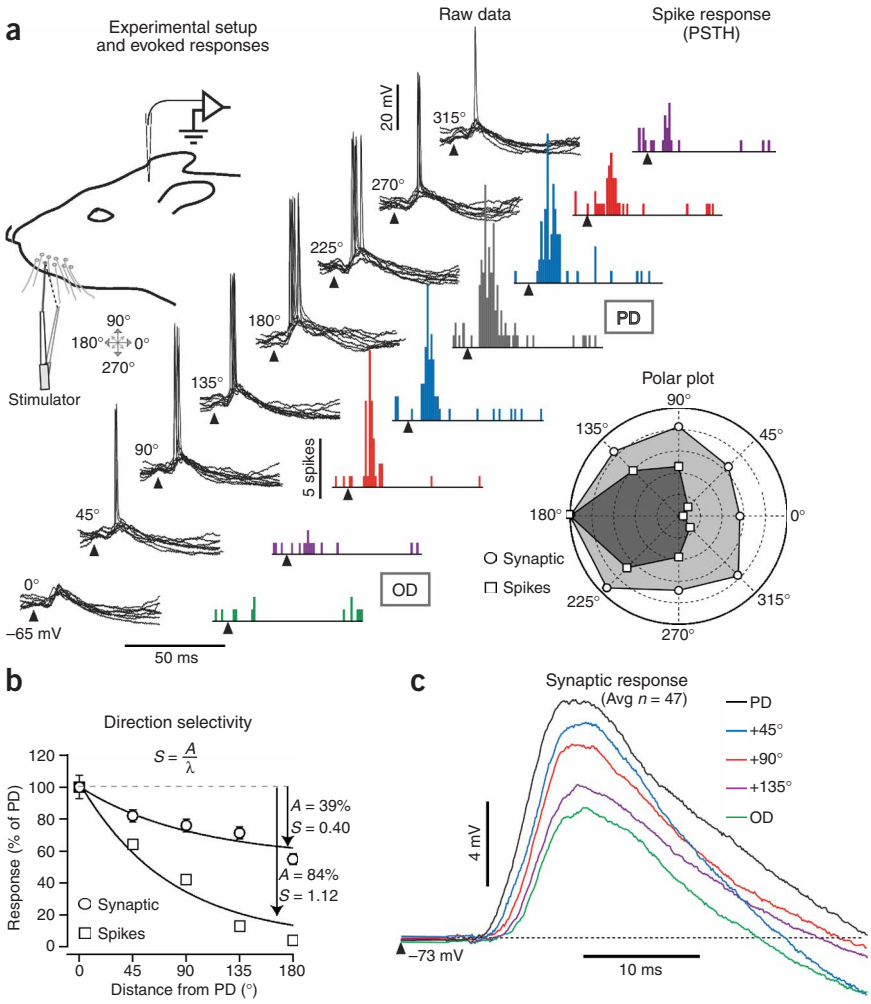

Figure 1 Direction selectivity in layer 4 barrel neurons. (**a**) The angular direction of whisker deflection was arbitrarily set so that caudal deflections corresponded to 0° and dorsal deflections to 90°. Superimposed single responses ('Raw data', $n = 8$) are shown for each direction at a slightly depolarized V_m (−65 mV, +0.2 nA). Arrowheads indicate stimulus onset. Spike responses to all trials ($n = 58$) for each direction were accumulated in the peristimulus spike histograms (PSTH). The spike response for this cell, expressed as spikes per stimulus, and the amplitude of the synaptic response (in mV, measured from the baseline preceding the stimulus) were normalized to the preferred direction (PD) response and are shown in the polar plot. (**b**) The normalized spike and synaptic response magnitude were plotted as function of distance from the preferred direction. In doing so, data from directions equidistant from the preferred direction, in increments of 45°, were collapsed together. The data was fit with a decaying exponential function, and the percentage amplitude decay (A) from the preferred direction and the decay constant (λ) of the fit were used to calculate the selectivity index (S). The spike response ($S = 1.12$) was more selective than the synaptic response ($S = 0.40$). (**c**) The amplitude and dV/dt of the averaged synaptic responses recorded at rest (−73 mV) decreased from the preferred direction (11.0 mV, 2.1 mV ms^{-1}) to the opposite direction (OD; 6.0 mV, 1.3 mV ms^{-1}).

response (8.2 mV). The number of spikes per stimulus and the synaptic response peak amplitude decreased as the direction of deflection deviated from the preferred direction, and both were lowest for the opposite direction (0.05 spikes per stimulus, 5.6 mV; **Fig. 1a**). The spike output was more sensitive to direction than was the underlying synaptic response amplitude, measured from the resting V_m (−72 mV). This is shown in a polar plot (**Fig. 1a**) by the larger direction-dependent differences in spike output than in the amplitude of the synaptic response.

To quantify direction selectivity, we did not use the parameter values from Gaussian fits to the response magnitude, as is commonly done in other sensory systems[18], because response variability led to poor-quality fits[19]. Because response magnitude decreased mainly as a function of the relative angular difference with respect to the preferred direction, we collapsed the responses from directions equidistant from the preferred direction. For example, responses to deflections to 225° and 135° (**Fig. 1a**, blue) were averaged together because they both diverge 45° from the preferred direction. This procedure generated five values of response magnitude (preferred direction, 45°, 90°, 135° and opposite direction), measured in spikes per stimulus for the spike response and in mV for the synaptic response, that were accurately described by a decaying exponential when plotted as a function of distance from the preferred direction (**Fig. 1b**). To compare the selectivity of synaptic and spike response magnitude, we used a direction selectivity index (S), calculated as the percent decay in amplitude (A) from the preferred direction; that is, amplitude = (preferred direction − nonpreferred direction)/preferred direction, divided by the decay constant of the fit exponential (λ). Thus, this ratio S is a measure of the percent decrease in response magnitude for each degree away from the preferred direction, and it reflects the tuning properties of individual cells better than the more commonly used direction index in which the responses to non-preferred directions are averaged together. For this example cell (**Fig. 1**), the spike response magnitude was more selective ($A = 84\%$, $\lambda = 75°$, $S = 1.12$) than the underlying synaptic response at –65 mV ($A = 39\%$, $\lambda = 97°$, $S = 0.40$), which agrees with the population data[19]. Finally, as the direction diverged from the preferred direction, there was a progressive decrease in response amplitude and a slight increase in onset latency clearly visible in the responses recorded at rest (**Fig. 1c**, −73 mV, 0 nA).

Estimations of membrane conductance and reversal potential

To elucidate the composition of the synaptic responses, a subset of cells ($n = 14$) was recorded in the presence of QX-314 (75 mM, added to the pipette solution), which blocks voltage-gated sodium channels[20] as well as potassium and calcium conductances[21] and allows the study of synaptic responses evoked at depolarized V_m that are well above spike threshold (**Fig. 2a**). Whisker deflections were coupled with five different levels of current injection that started 200 ms before the deflection to avoid capacitive artifacts. Using the V_m values obtained during current injection, we estimated (**Supplementary Methods**) the total conductance of the cell (G_{total}) and the apparent reversal potential of the synaptic response (V_{rev}). These estimations were accurate because, in all cells, (i) it was possible to fully reverse the synaptic responses both in the depolarizing and the hyperpolarizing direction

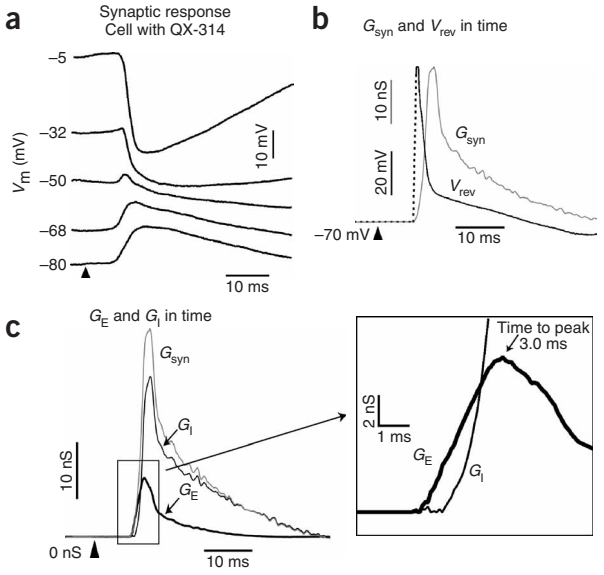

Figure 2 Excitatory and inhibitory conductances underlying the synaptic responses. (**a**) Synaptic responses of a layer 4 cell at five holding V_m values (−5 to −80 mV) to preferred direction whisker deflections. Arrowhead indicates stimulus onset. The magnitude and polarity of the response is V_m dependent. (**b**) G_{syn} and V_{rev} were calculated at every time point during the response. V_{rev} was not calculated for the baseline ($G_{syn} = 0$) and for the first few points of the response and is represented as a dotted line. (**c**) Decomposition of G_{syn} (light gray) into G_E (thick black line) and G_I (thin black line); see Methods. The inset shows the early part of the change in G_E and G_I on a larger scale to illustrate their relative changes in amplitude over time.

(**Fig. 2a**); (ii) the responses were obtained from at least five V_m values, and the behavior of the V_m was linear in all cases; and (iii) the time constants of all cells were similar (~7 ms; see ref. 5). The value of resting conductance (G_{rest}) was estimated as the average G_{total} for the 50 ms preceding the synaptic response. The value of G_{rest} was subtracted from G_{total} during the response to obtain the change in conductance due to the synaptic input, or the synaptic conductance (G_{syn}).

Synaptic conductance and reversal potential over time

We calculated G_{syn} and V_{rev} for every time point during the synaptic response. For baseline, when G_{syn} is zero, and for the first data points of the rising of G_{syn}, where the estimation of V_{rev} is inherently variable, we did not calculate V_{rev}, which is represented as a dotted line. For the example cell shown (**Fig. 2b**), the value of V_{rev} reached a peak of −5 mV (at 7.5 ms latency from stimulus onset) followed by a fast drop to −60 mV (at about 12 ms) and then a slow decay toward −80 mV. The value of G_{syn} increased to a maximum of 35.0 nS coinciding with the V_{rev} value of −60 mV. Following studies in visual[1,18,22] and auditory[3,23] cortices, we assumed that the synaptic response was primarily composed of glutamatergic (AMPA) synaptic inputs with a reversal potential at 0 mV and GABAergic ($GABA_A$) synaptic inputs with a reversal potential at −75 mV. On the basis of these assumptions, we decomposed G_{syn} into excitatory (G_E) and inhibitory (G_I) conductances (**Fig. 2c**) using the equation of the parallel conductance model of the membrane[24,25]. This method has been widely done in other systems[1,3,18,23] (see Methods). The amplitude of G_I was larger than that of G_E, but more importantly, the two conductances showed differences in time course (**Fig. 2c**, inset) that were direction dependent (see below). We measured the latency to peak of G_E and G_I from the onset of the change in synaptic conductance. For the cell shown, G_E reached its peak at 3.0 ms and G_I at 4.2 ms (**Fig. 2**). The importance of the relative strength of the conductances early in the response was illustrated by the fact that most of the spike response to the preferred direction occurred before the peak in G_{syn} and when G_{syn} was dominated by G_E. (**Supplementary Fig. 1**).

Synaptic conductances as a function of direction

In order to determine the nature of the synaptic inputs underlying direction selectivity, we estimated the synaptic conductances as a function of the direction of whisker deflection. The decrease in synaptic response amplitude as the direction deviated from the preferred direction may be due to (i) a selective decrease in excitation, (ii) a selective increase in inhibition or (iii) a decrease of both inputs, whereby selectivity would be a reflection of total synaptic input. In addition, systematic differences in the relative timing of excitation and inhibition may have a critical role in determining the amplitude and shape of the synaptic response.

Whisker-evoked responses were recorded for different directions and five holding potentials with pipettes containing QX-314 (**Fig. 3a**). Direction-dependent differences in the synaptic response were most

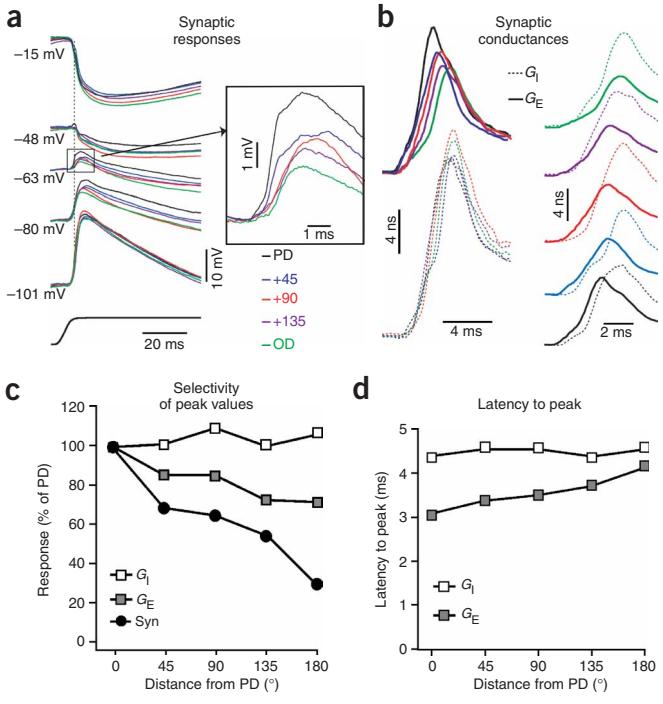

Figure 3 Timing of excitatory and inhibitory conductances as a function of direction. (**a**) Synaptic responses to whisker deflections for an individual cell at five holding potentials (−15 mV, −48 mV, −63 mV, −80 mV and −101 mV). Inset shows responses evoked at −63 mV on a larger scale to show differences in the amplitude and time course of the synaptic response. (**b**) Continuous plots of G_I (dotted lines) and G_E (solid lines) show that the latency to peak and peak amplitude of G_I did not change appreciably with direction, whereas the latency to peak and peak amplitude of G_E slightly decreased as the direction deviated from the preferred direction. This generated a clear direction-dependent temporal shift between G_E and G_I (right column). (**c**) The synaptic response (circles) was selective for the preferred direction, whereas G_I was not selective, and G_E was only modestly selective. (**d**) The plot of latency to peak shows a constant value for G_I (around 4.4 ms) and a systematic increase for G_E (from 3.1 to 4.0 ms).

pronounced at values of V_m near spike threshold. Responses at these V_m values are functionally relevant because the underlying net synaptic current is directly translated into spike output, which is well tuned for direction (**Fig. 3a**; inset shows responses from −63 mV; spike threshold was −56 mV for this cell as measured before blockade of spikes by QX-314). Both conductances showed a small decrease in amplitude for directions away from the preferred direction, but only G_E showed a concomitant change in time course (**Fig. 3b**). This change in timing resulted in a G_E that clearly preceded G_I for the preferred direction (**Fig. 3b**, right) but not for the opposite direction (**Fig. 3b**, right). The peak amplitudes of the estimated G_I and G_E (**Fig. 3c**) were highest for the preferred direction and decayed slightly at non-preferred directions. The amplitude of the synaptic response (**Fig. 3c**) was clearly more selective than the underlying conductances, suggesting that the tuning of the amplitude of the inputs may not be enough to account for the selectivity of the synaptic response. The other potential mechanism to generate response selectivity is the relative timing of the inputs. Indeed, as already visible in the average conductance traces (**Fig. 3b**), the time to peak of G_I changed little across directions (range 4.4–4.6 ms, **Fig. 3d**), whereas the time to peak of G_E progressively increased (**Fig. 3d**) with increasing distance from the preferred direction.

To validate the synaptic conductance estimates, we used their values to reconstruct the V_m responses. We predicted the V_m responses for the first 25 ms, because we are confident that the response is primarily mediated by ionotropic glutamatergic and $GABA_A$ conductances in this time window. The predictions closely matched the actual values for this cell (average RMS error: 0.28 ± 0.5, mean ± s.d.)[3]. Another example cell (**Supplementary Fig. 2**) shows that the predictions captured the tuning at the V_m near threshold.

Our data show that the amplitude and the time course of both G_E and G_I change with direction. However, the measurements of peak amplitude and latency to peak are static measures, and they do not capture the dynamics of G_E and G_I over time, nor do they provide information on synaptic current (**Fig. 3**). To characterize the relative amplitudes of G_E and G_I during the response, we calculated the amount of fractional excitatory input (FG_E; ref. 3) over time as $FG_E = G_E/(G_E + G_I)$. Thus, an FG_E value of 1 indicates a purely excitatory synaptic input (with an associated value of estimated V_{rev} of 0 mV) and a FG_E value of 0 indicates a purely inhibitory input (with an associated value of estimated V_{rev} of −75 mV). This procedure is illustrated for an example cell (**Fig. 4**). The cell was also recorded with QX-314 in the pipette, and responses to whisker deflection in the eight different directions were obtained at five different V_m values (**Fig. 4a**). From those V_m values we estimated the underlying G_E and G_I (**Fig. 4a**), which were very similar in amplitude and time course to those in **Figure 3,** and we calculated the value of FG_E (**Fig. 4b**). Differences in the value of FG_E across directions occurred only during the first 5 ms of the response. The conductances were balanced thereafter. During the response to the preferred direction, FG_E reached 60% 1 ms after the onset of the response, then decayed below 50% after 3 ms, and reached 40% at around 7 ms. The responses to the other directions were always below 50%, and all directions reached a common value of 40% at 7 ms, after which they decreased slightly.

The values of the synaptic conductances are independent of V_m, but the polarity and amplitude of the currents they conduct are dependent on the V_m of the cell. For example, a depolarizing synaptic event may not be excitatory if the V_{rev} of the synaptic response (that is, the balance of the excitatory and inhibitory synaptic conductances) is below spike threshold. Because G_E and G_I overlap during the synaptic response, in order to understand whether their combined action has a net excitatory or inhibitory effect, it is critical to determine the net amount of

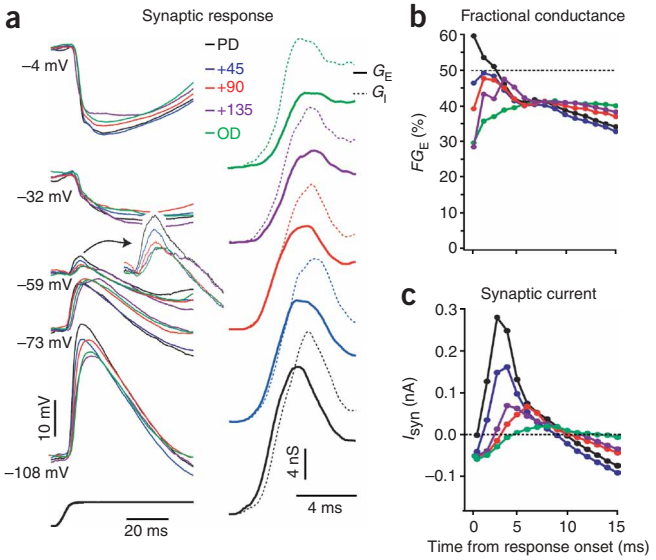

Figure 4 Dynamics of G_E and G_I. (**a**) Synaptic responses to whisker deflections for an individual cell at five holding potentials (−4 mV, −32 mV, −59 mV, −73 mV and −108 mV). Responses evoked at −59 mV are shown at a larger scale (indicated by arrow) to show differences in synaptic response amplitude and time course. Continuous plots of G_I (right column, dotted lines) and G_E (solid lines) show a similar amplitude and temporal relation between G_E and G_I as in the example in **Figure 3**. (**b**) Fractional G_E (FG_E) as a function of time for the different directions; time resolution is 1 ms. FG_E reached 60% in the first 1 ms and decayed rapidly; for all directions, FG_E was relatively stable at 40% after 7–9 ms. (**c**) Total synaptic current (I_{syn}) over time. I_{syn} was calculated at threshold V_m for this cell (−55 mV), and therefore it is excitatory for positive values and inhibitory for negative values. The tuning of I_{syn} was similar to that of the synaptic response nearest spike threshold.

synaptic current generated at a V_m near spike threshold. The value of I_{syn} at V_{thr} was estimated as $I_{syn} = G_{syn}(V_m - V_{thr})$, using a V_{thr} of −55 mV (ref. 19); consequently, positive values of I_{syn} indicate a net excitatory current and vice versa. The average spike threshold was difficult to determine before the action of QX-314; therefore, we arbitrarily chose the average value for cells recorded without QX-314. For this cell early in the response, there were large differences in the amplitude of the currents with a peak excitatory I_{syn} (0.3 nA) for the preferred direction at 4 ms that was twice the amplitude of the current during the response to 45° away (1.5 nA) and six times the current flowing for deflections 90° away (0.5 nA; **Fig. 4c**). However, by 7 ms the net synaptic current was only weakly excitatory and was similar for all directions (0.2–0.5 nA). Thus, the direction-dependent temporal relationship between G_E and G_I results in a direction-dependent net excitatory current that determines the selectivity of the synaptic response and the spike output of the neuron. We will show below that this was the general rule for the population.

We quantified the static and dynamic parameters described above for the population. The peak amplitude of both G_I and G_E (**Fig. 5a**) showed weak direction selectivity (G_I: $S = 0.44$ and G_E: $S = 0.68$) and did not reflect the selectivity of the synaptic response ($S = 0.95$; **Fig. 5a**). The latency to the peak of G_E progressively increased with increasing distance from the preferred direction, whereas that of G_I was relatively constant (**Fig. 5b**), demonstrating that the systematic change in timing between G_E and G_I as a function of deflection direction was a general property of our population. Similar to the cell in **Figure 4**, only during the initial 5 ms of the response was the value of FG_E for the population (**Fig. 5c**) direction dependent. The population value of I_{syn} (**Fig. 5d**)

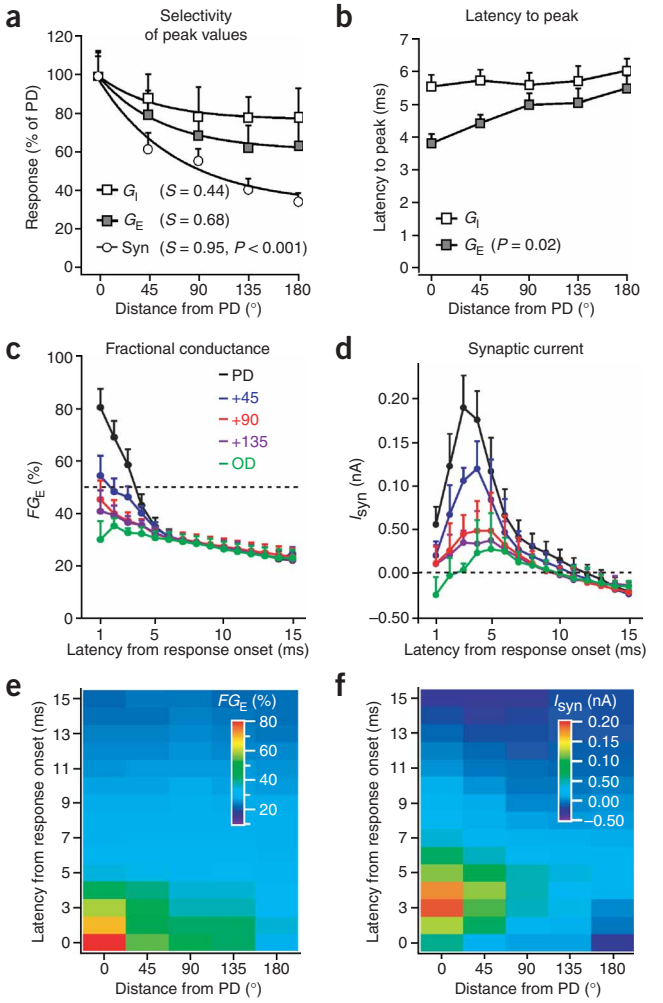

Figure 5 Population values. (**a**) For the population of cells recorded with QX-314, direction tuning of the synaptic response (circles; measured at –63 mV) was sharper ($S = 0.95$, $F = 3.6$, one-way ANOVA, $P < 0.001$) than the tuning of G_I (open squares) and G_E (filled squares; $S = 0.44$ and 0.68, respectively). (**b**) The latency to peak of G_E and G_I for the population showed a direction-dependent systematic phase shift of excitation with respect to inhibition. (**c**) Fractional G_E (FG_E) during the course of the synaptic response for the different directions; time resolution is 1 ms. FG_E was strongly direction dependent during the first 5 ms of the response. After 5 ms, FG_E for all directions decayed slowly from 35%. (**d**) Total synaptic current (I_{syn}) over time. I_{syn} was calculated at the mean spike threshold V_m for the population (−55 mV), and therefore it is excitatory for positive values and inhibitory for negative values. It shows strong direction selectivity during the first 7–8 ms. (**e**) Direction selectivity of FG_E. The values of FG_E (in pseudocolor) shown in **c** were plotted for all directions (*x*-axis) and over time (*y*-axis) with 1-ms temporal resolution. In the first 1 ms, FG_E was strongly direction-dependent (preferred direction = 80%, opposite direction = 30%) but was not after 5 ms (preferred direction = opposite direction = 32%). (**f**) Direction selectivity of I_{syn}. Plot as in **e**. It is clear that I_{syn} was very direction selective between 2 and 5 ms but not thereafter. Error bars, s.e.m.

was excitatory for the initial 8–9 ms of the response but showed a clear peak only for the preferred direction and 45° away from it, indicating that directions 90° or more away from the preferred direction generate a very weak excitatory net current reflecting their low probability of spiking. To illustrate the direction dependence of FG_E, we plotted FG_E as a function of direction and time (**Fig. 5e**). This ratio was strongly direction selective in the first 1 ms of the response (from 80% for the preferred direction to 30% for the opposite direction) and was no longer selective after 5 ms from response onset; that is, the ratio of G_E and G_I did not change with direction. In the case of I_{syn} calculated at threshold V_m (**Fig. 5f**), the maximum direction selectivity occurred at 3 ms after the onset of the response, but I_{Syn} was no longer selective after 7 ms.

DISCUSSION

Our results show that the selectivity of the synaptic response of barrel neurons to the direction of whisker deflection is associated with a weak selectivity of the amplitude of excitatory and inhibitory inputs and, more importantly, a systematic shift in the temporal relation between excitation and inhibition. Inhibition is largest for the preferred direction, but because of the direction-dependent phase shift of excitation relative to inhibition, it actually sharpens the tuning of the response. This result is comparable to what has been shown for the velocity sensitivity of these cells[5]; that is, inhibition imposes a limited time window, or a 'window of opportunity'[26,27] in which excitatory inputs are capable of evoking a spike response.

Contrary to the visual system, where orientation selectivity emerges in layer 4 from specific convergence patterns of non-tuned thalamic inputs, in the somatosensory system, direction selectivity is already present in the primary afferents innervating the whisker follicles. The selectivity of the primary afferents is due to the restricted distributions of receptors around the follicle[9,28,29]. The afferents impose their selectivity on the neurons of the principal trigeminal nucleus, which in turn project to neurons in the ventroposterior medial (VPm) nucleus, where a map of shifting direction preference emerges along the length of the barreloids[30]. Neurons in the VPm nucleus inherit trigeminal direction preference because (i) the degree of convergence of prethalamic input[31,32] is small, (ii) there is a similar number of neurons between VPm barreloids and trigeminal barrelettes (~200) and (iii) trigeminal axons have restricted terminal fields in thalamus[33,34]. Indeed, trigeminal and thalamic cells show similar direction selectivity[35]. In addition, VPm cells with similar direction selectivity are clustered within barreloids, as shown by the strong correlation of direction preference between neighboring cells[30] and the dependency on the direction of whisker deflection of the amplitude of local field potential responses along the depth of the VPm[36].

In contrast, in barrel cortex, the divergence of thalamic input, the extensive dendritic arborization of layer 4 cells and the rich recurrent circuitry seem to preclude a simple anatomical scheme for the conservation of direction preference. The details of the distribution of thalamic terminal fields in the barrel cortex are not fully understood. However, using spike-triggered averaging of field potentials evoked by single barreloid neurons, others[11] have shown that the axonal terminal potential, which reflects the impact of a single thalamic input[37], varies among locations within the barrel, suggesting that the density of thalamocortical synapses within its terminal field is not uniform. In addition, the same authors have shown that the impact of a single thalamic input (the amplitude of the axon terminal potential) correlates with the degree of similarity between its direction preference and that of local barrel neurons and, furthermore, that thalamic neurons with similar direction preference converge on regions of the barrel sharing that preference. Finally, the likelihood of functional connectivity between a thalamic neuron and a regular spiking cell in the aligned barrel is higher if the two cells have a similar direction preference[4]. In fact, direction tuning is shared by individual neurons within small vertical domains within the barrel[11], which are similar in diameter to proposed functional minicolumns (<100 μm)[38]. Such domains are not represented systematically along the horizontal axis of the barrel, as

shown by the abrupt transitions of direction preference in tangential penetrations[11]. On the basis of the functional mapping results from cortex[11] and thalamus[30] discussed above, the hypothesis was formulated that direction tuning in layer 4 barrel neurons is preserved owing to spatial gradients of convergent thalamocortical connections and that spatial and temporal summation of overlapping terminal fields with different innervation densities generates direction selectivity[11,30]. Such a mechanism predicts that excitatory inputs are tuned for direction. Our data, however, show that the amplitude of the excitatory conductances changes only modestly with direction and that all directions of deflection evoke subthreshold depolarizing synaptic responses from resting V_m values. More importantly, the latency to onset of the synaptic response indicates that barrel neurons receive monosynaptic thalamic input from deflections in all directions (that inputs from different directions of deflection reach layer 4 neurons has been shown before)[4]. In addition, it has been shown that neighboring thalamic cells generate widely differing spatiotemporal patterns of monosynaptic activation within layer 4 (ref. 39), again arguing against the preservation of direction tuning only on the basis of anatomical maps of thalamic input.

A similar mechanism to the one proposed here for direction was originally proposed for somatotopy[40]. These authors showed that the timing of excitation against a relatively constant inhibitory input is critical in determining which synaptic inputs generate an output in barrel cortex cells, thus determining the size of the suprathreshold receptive field from a spatially much larger subthreshold receptive field. In their description, changes in timing were somewhat related to the distance from the principal whisker. Here we have shown that a fine and systematic shift in timing is a key component underlying direction selectivity.

What underlies the direction-dependent timing differences? One hypothesis is that the degree of synchronization of thalamic output is selectively modulated by direction[41]. In such conditions, rather than depending on precise anatomical maps, the impact of thalamic input in cortex depends on the direction-dependent level of synchronization of thalamic populations. This hypothesis proposes a mechanism similar to that underlying the responses to different deflection velocities[5,26,27]. In the case of velocity, the synchronization hypothesis is supported by extracellular recordings from thalamic and cortical cells showing that increasing whisker deflection velocity reduces the duration of the thalamic response without changing the total spike count, and therefore thalamic output synchrony increases with deflection velocity[27]. In contrast, for the case of direction, as the whisker deflection deviates from the preferred direction, the response of thalamic cells is primarily reduced in the total number of spikes and not in the shape of PSTH. However, although the spike number is greatly reduced at nonpreferred directions, there is a slight increase in the latency to spiking as the direction diverges from the preferred direction. Thus, although thalamic input synchrony probably contributes to direction tuning, it is probably not the primary mechanism in cortex.

Another common hypothesis regarding the tuning of neurons in primary sensory cortices to specific stimulus features involves a nonspecific local inhibitory input that limits the ability of weaker excitatory inputs, such as that associated with a non-optimal stimulus, to bring a cell to threshold for action potential generation. In such models, inhibition enhances the selectivity of an already-tuned excitatory input. However, our data show that excitatory inputs are only weakly tuned for direction. Instead, excitation has a progressively slower time course with respect to the inhibitory input. Therefore, in barrel neurons, inhibition seems critical in establishing, rather than merely enhancing, direction selectivity. This is consistent with the fact that direction selectivity increases as the velocity of whisker deflection decreases[41]. Inhibitory cells in the barrel are less sensitive to the velocity of the whisker deflection; consequently, the presumed increase in the latency to peak of the excitatory input should effectively increase the ability of the inhibitory input, which is less sensitive to the velocity of the deflection[4], to filter only the most proximal excitatory inputs.

Although nonspecific inhibition may have a prominent role, it does not explain the time shift in excitation. One source may be a decrease in thalamic synchrony as the direction deviates from the preferred; however, if this were solely responsible, it should have produced a simple systematic reduction in the slope of the excitatory conductance, which was not the case. Another possible source of the temporal properties of the excitatory inputs is the anatomical arrangement of the synaptic inputs on the dendrites. For example, the distribution of preferred-direction synaptic inputs may be primarily on proximal dendrites, and as the direction diverges from the preferred, the distribution of the associated synaptic inputs may have progressively more distal bias. The temporal shift between excitation and inhibition may then be simply a product of the direction-dependent temporal delays associated with the electrotonic conduction of the excitatory inputs to the soma. This arrangement would be highly dependent on the ability of the inhibitory inputs to maintain selectivity by limiting the ability of distal dendritic excitatory inputs to evoke a response. Disruptions within local inhibitory networks should then have deleterious effects on selectivity, which is consistent with the fact that decreases in intracortical inhibition[42] have been shown to reduce the stimulus selectivity of primary sensory cortex cells in senescent animals[43]. This hypothesis is also highly dependent on the time it takes a dendritic input to affect the V_m at the soma. Recent studies have placed varying levels of importance on the role of dendritic input location[44,45]; however, those studies have primarily focused on the decay of the amplitude of the input.

In conclusion, we have elucidated the dynamics of the excitatory and inhibitory inputs underlying the direction selectivity of barrel cortex layer 4 cells and identified the timing of the inputs as the key element; however, future work is needed to resolve the source of the temporal properties of the inputs driving the feature selectivity of these cells.

METHODS

Surgery. Experiments were conducted in accordance with the ethical guidelines of the US National Institutes of Health and with the approval of the Institutional Animal Care and Use Committee of the University of Pennsylvania. Adult male Sprague-Dawley rats (350–450 g) were anesthetized with pentobarbital (50 mg kg^{-1} intraperitoneal) and buprenorphine (0.03 mg kg^{-1} subcutaneous) was administered to provide additional analgesia. Surgery and anesthesia procedures have been described previously[5,16]. At the end of each experiment, animals were perfused intracardially with 4% paraformaldehyde, and brains were removed and postfixed overnight in the same fixative. Tissue sections were processed for neurobiotin using Cy3-conjugated streptavidin (Jackson ImmunoResearch) as described elsewhere[5].

Intracellular recordings. Intracellular recordings were performed, as described previously[5,19], with glass micropipettes filled with 3 M potassium acetate ($n = 23$) or with 75 mM QX-314 added ($n = 14$). In both cases, neurobiotin (Vector Laboratories) 2% was added to the pipette solution. QX-314 primarily blocks fast voltage-gated Na channels. The resting input resistance was 27 ± 8 MΩ for cells recorded without QX-314 and 54.6 ± 16 MΩ, (mean ± s.d.) for cells recorded with QX-314. All cells included in the database were located at a subpial depth between 450–850 μm as indicated on the scale of the micromanipulator and confirmed histologically as also shown previously[5]. All cells had stable membrane potential (V_m) below −60 mV for at least 20 min and overshooting action potentials. All cells had response onset latencies from whisker stimulation below 7.5 ms and were therefore considered to receive

monosynaptic thalamic input[40]. All cells were of the regular spiking electrophysiological category[46,47].

All data analyses were done offline using Igor Pro (Wavemetrics). An analysis of variance (ANOVA) was used to compare more than two groups, and the Tukey HSD post-hoc test was used for pairwise comparisons.

Whisker stimulation. The principal whisker and preferred direction were determined, as described previously, as the whisker or direction that evoked, from a slightly depolarized V_m, the most spikes or the largest synaptic response. The principal whisker was repeatedly deflected in eight randomly interleaved directions, separated by 45°, using a velocity of 1,300° s^{-1} (acceleration, 7.8 × 10^5 deg s^{-2}). Caudal deflections are referred to as the 0° direction, rostral deflections as 180°, dorsal deflections as 90° and ventral deflections as 270°. All stimuli were 100 ms ramp and hold, and for trials at depolarized and hyperpolarized V_m values, current pulses were applied at least 200 ms before whisker stimuli to ensure that the V_m had reached steady state to avoid capacitive artifacts. The driving voltage on the piezos was adjusted so that the amplitude of the displacement was 1.0 mm, or 5.7°, for all directions and the separation between each angular displacement was 45°. An optoelectronic device was used to record the movement of the stimulator in each direction. Since the optoelectronic device measures movement only in one plane, the stimulator was rotated by 45° after a given angular deflection was recorded so that all eight angles moved in the same direction/plane when being recorded. The velocity of the deflection was approximately 1,300° s^{-1} for all directions (**Supplementary Fig. 3**).

Note: Supplementary information is available on the Nature Neuroscience website.

ACKNOWLEDGMENTS

The authors would like to thank R. Traub for intellectual input throughout the preparation of this manuscript, E. Garcia de Yebenes for her technical assistance and A. Reid and J. Cardin for their useful comments. Sponsored by the Human Frontier Science Program Organization.

COMPETING INTERESTS STATEMENT

The authors declare that they have no competing financial interests.

Published online at http://www.nature.com/natureneuroscience/
Reprints and permissions information is available online at http://npg.nature.com/reprintsandpermissions/

1. Monier, C., Chavane, F., Baudot, P., Graham, L.J. & Fregnac, Y. Orientation and direction selectivity of synaptic inputs in visual cortical neurons: a diversity of combinations produces spike tuning. *Neuron* **37**, 663–680 (2003).
2. Schummers, J., Marino, J. & Sur, M. Synaptic integration by V1 neurons depends on location within the orientation map. *Neuron* **36**, 969–978 (2002).
3. Wehr, M. & Zador, A.M. Balanced inhibition underlies tuning and sharpens spike timing in auditory cortex. *Nature* **426**, 442–446 (2003).
4. Bruno, R.M. & Simons, D.J. Feedforward mechanisms of excitatory and inhibitory cortical receptive fields. *J. Neurosci.* **22**, 10966–10975 (2002).
5. Wilent, W.B. & Contreras, D. Synaptic responses to whisker deflections in rat barrel cortex as a function of cortical layer and stimulus intensity. *J. Neurosci.* **24**, 3985–3998 (2004).
6. Miller, K.D., Pinto, D.J. & Simons, D.J. Processing in layer 4 of the neocortical circuit: new insights from visual and somatosensory cortex. *Curr. Opin. Neurobiol.* **11**, 488–497 (2001).
7. Douglas, R.J. & Martin, K.A. Neuronal circuits of the neocortex. *Annu. Rev. Neurosci.* **27**, 419–451 (2004).
8. Simons, D.J. & Carvell, G.E. Thalamocortical response transformation in the rat vibrissa/barrel system. *J. Neurophysiol.* **61**, 311–330 (1989).
9. Lichtenstein, S.H., Carvell, G.E. & Simons, D.J. Responses of rat trigeminal ganglion neurons to movements of vibrissae in different directions. *Somatosens. Mot. Res.* **7**, 47–65 (1990).
10. Mountcastle, V.B. Modality and topographic properties of single neurons of cat's somatic sensory cortex. *J. Neurophysiol.* **20**, 408–434 (1957).
11. Bruno, R.M., Khatri, V., Land, P.W. & Simons, D.J. Thalamocortical angular tuning domains within individual barrels of rat somatosensory cortex. *J. Neurosci.* **23**, 9565–9574 (2003).
12. Staiger, J.F. *et al.* Functional diversity of layer IV spiny neurons in rat somatosensory cortex: quantitative morphology of electrophysiologically characterized and biocytin labeled cells. *Cereb. Cortex* **14**, 690–701 (2004).
13. Petersen, C.C. & Sakmann, B. The excitatory neuronal network of rat layer 4 barrel cortex. *J. Neurosci.* **20**, 7579–7586 (2000).
14. Jensen, K.F. & Killackey, H.P. Terminal arbors of axons projecting to the somatosensory cortex of the adult rat. I. The normal morphology of specific thalamocortical afferents. *J. Neurosci.* **7**, 3529–3543 (1987).
15. Feldmeyer, D., Egger, V., Lubke, J. & Sakmann, B. Reliable synaptic connections between pairs of excitatory layer 4 neurones within a single 'barrel' of developing rat somatosensory cortex. *J. Physiol. (Lond.)* **521**, 169–190 (1999).
16. Higley, M.J. & Contreras, D. Nonlinear integration of sensory responses in the rat barrel cortex: an intracellular study *in vivo*. *J. Neurosci.* **23**, 10190–10200 (2003).
17. Simons, D.J., Carvell, G.E., Hershey, A.E. & Bryant, D.P. Responses of barrel cortex neurons in awake rats and effects of urethane anesthesia. *Exp. Brain Res.* **91**, 259–272 (1992).
18. Carandini, M. & Ferster, D. Membrane potential and firing rate in cat primary visual cortex. *J. Neurosci.* **20**, 470–484 (2000).
19. Wilent, W.B. & Contreras, D. Stimulus-dependent changes in spike threshold enhance feature selectivity in rat barrel cortex neurons. *J. Neurosci.* **25**, 2983–2991 (2005).
20. Connors, B.W. & Prince, D.A. Effects of local anesthetic QX-314 on the membrane properties of hippocampal pyramidal neurons. *J. Pharmacol. Exp. Ther.* **220**, 476–481 (1982).
21. Mulle, C., Steriade, M. & Deschenes, M. The effects of QX314 on thalamic neurons. *Brain Res.* **333**, 350–354 (1985).
22. Martinez, L.M., Alonso, J.M., Reid, R.C. & Hirsch, J.A. Laminar processing of stimulus orientation in cat visual cortex. *J. Physiol. (Lond.)* **540**, 321–333 (2002).
23. Tan, A.Y., Zhang, L.I., Merzenich, M.M. & Schreiner, C.E. Tone-evoked excitatory and inhibitory synaptic conductances of primary auditory cortex neurons. *J. Neurophysiol.* **92**, 630–643 (2004).
24. Hodgkin, A.L. & Huxley, A.F. A quantitative description of membrane current and its application to conduction and excitation in nerve. *J. Physiol. (Lond.)* **117**, 500–544 (1952).
25. Johnston, D. & Wu, S.M.S. *Foundations of Cellular Neurophysiology* (MIT Press, Cambridge, Massachusetts, 1996).
26. Pinto, D.J., Hartings, J.A., Brumberg, J.C. & Simons, D.J. Cortical damping: analysis of thalamocortical response transformations in rodent barrel cortex. *Cereb. Cortex* **13**, 33–44 (2003).
27. Pinto, D.J., Brumberg, J.C. & Simons, D.J. Circuit dynamics and coding strategies in rodent somatosensory cortex. *J. Neurophysiol.* **83**, 1158–1166 (2000).
28. Shoykhet, M., Doherty, D. & Simons, D.J. Coding of deflection velocity and amplitude by whisker primary afferent neurons: implications for higher level processing. *Somatosens. Mot. Res.* **17**, 171–180 (2000).
29. Zucker, E. & Welker, W.I. Coding of somatic sensory input by vibrissae neurons in the rat's trigeminal ganglion. *Brain Res.* **12**, 138–156 (1969).
30. Timofeeva, E., Merette, C., Emond, C., Lavallee, P. & Deschenes, M. A map of angular tuning preference in thalamic barreloids. *J. Neurosci.* **23**, 10717–10723 (2003).
31. Deschenes, M., Timofeeva, E. & Lavallee, P. The relay of high-frequency sensory signals in the Whisker-to-barreloid pathway. *J. Neurosci.* **23**, 6778–6787 (2003).
32. Castro-Alamancos, M.A. Properties of primary sensory (lemniscal) synapses in the ventrobasal thalamus and the relay of high-frequency sensory inputs. *J. Neurophysiol.* **87**, 946–953 (2002).
33. Veinante, P. & Deschenes, M. Single- and multi-whisker channels in the ascending projections from the principal trigeminal nucleus in the rat. *J. Neurosci.* **19**, 5085–5095 (1999).
34. Williams, M.N., Zahm, D.S. & Jacquin, M.F. Differential foci and synaptic organization of the principal and spinal trigeminal projections to the thalamus in the rat. *Eur. J. Neurosci.* **6**, 429–453 (1994).
35. Minnery, B.S., Bruno, R.M. & Simons, D.J. Response transformation and receptive-field synthesis in the lemniscal trigeminothalamic circuit. *J. Neurophysiol.* **90**, 1556–1570 (2003).
36. Temereanca, S. & Simons, D.J. Local field potentials and the encoding of whisker deflections by population firing synchrony in thalamic barreloids. *J. Neurophysiol.* **89**, 2137–2145 (2003).
37. Swadlow, H.A. & Gusev, A.G. The influence of single VB thalamocortical impulses on barrel columns of rabbit somatosensory cortex. *J. Neurophysiol.* **83**, 2802–2813 (2000).
38. Mountcastle, V.B. Introduction. Computation in cortical columns. *Cereb. Cortex* **13**, 2–4 (2003).
39. Swadlow, H.A., Gusev, A.G. & Bezdudnaya, T. Activation of a cortical column by a thalamocortical impulse. *J. Neurosci.* **22**, 7766–7773 (2002).
40. Moore, C.I. & Nelson, S.B. Spatio-temporal subthreshold receptive fields in the vibrissa representation of rat primary somatosensory cortex. *J. Neurophysiol.* **80**, 2882–2892 (1998).
41. Lee, S.H. & Simons, D.J. Angular tuning and velocity sensitivity in different neuron classes within layer 4 of rat barrel cortex. *J. Neurophysiol.* **91**, 223–229 (2004).
42. Leventhal, A.G., Wang, Y., Pu, M., Zhou, Y. & Ma, Y. GABA and its agonists improved visual cortical function in senescent monkeys. *Science* **300**, 812–815 (2003).
43. Schmolesky, M.T., Wang, Y., Pu, M. & Leventhal, A.G. Degradation of stimulus selectivity of visual cortical cells in senescent rhesus monkeys. *Nat. Neurosci.* **3**, 384–390 (2000).
44. Magee, J.C. & Cook, E.P. Somatic EPSP amplitude is independent of synapse location in hippocampal pyramidal neurons. *Nat. Neurosci.* **3**, 895–903 (2000).
45. Williams, S.R. & Stuart, G.J. Dependence of EPSP efficacy on synapse location in neocortical pyramidal neurons. *Science* **295**, 1907–1910 (2002).
46. Connors, B.W. & Gutnick, M.J. Intrinsic firing patterns of diverse neocortical neurons. *Trends Neurosci.* **13**, 99–104 (1990).
47. Contreras, D. Electrophysiological classes of neocortical neurons. *Neural Netw.* **17**, 633–646 (2004).